dix of reference *5*). Most of the structures disappear in Fig. 3*c*, which is enlarged from Fig. 2*b* where the electric vector is along the minor axis.

The most likely interpretation of these results is that a magnetic field is present and is aligned predominately along the minor axis of M82. This field extends into the halo above and below the major axis to angular distances of 4.8 minutes of arc on the south side and 3.9 minutes of arc on the north side, which is the extent of the filamentary system shown in Fig. 1*b*. The distance of M82 is estimated to be $d = 9.8 \times 10^{24}$ cm (*2*), which gives the extent of the magnetic field as 4.4×10^3 parsec (1.3×10^{22} cm) from the plane of the galaxy on the south side and 3.9×10^3 parsec (1.2×10^{22} cm) from the plane on the north side.

It would seem that M82 may be the first galaxy in which large-scale magnetic field structure has actually been observed. Detailed mapping of the field is planned when more extensive polarization plates, taken in blue light at a variety of position angles, are available. The origin of the field can only be guessed, but it may have originally been present in the main body of the galaxy and have been drawn out by the plasma thrown poleward in the initial explosion along the minor axis.

Calculation of the energetics of the entire system (*2*) has shown that the average magnetic field strength probably lies between 10^{-5} and 10^{-6} gauss. The energies of the electrons causing the optical radiation are then exceedingly high, as shown by the following calculation.

A single relativistic electron of energy E moving in a field of strength $H_\perp$ perpendicular to the motion of the electron will radiate energy near frequency ν given by

$$\nu = 1.6 \times 10^{13} H_\perp E^2$$

where ν is in cycles per second, H is in gauss, and E is in Bev (10^9 ev). It is likely that ν for the optical synchrotron component of M82 is at least 10^{15} cy/sec as required by Figs. 1*b*, 2*a*, and 2*b*, and by the condition that the photoionization energy of the Hα recombination filaments comes from the synchrotron emission. This gives $E = 2.5 \times 10^3$ Bev if $H = 10^{-5}$ gauss and $E = 8 \times 10^3$ Bev if $H = 10^{-6}$ gauss—energies which are in the cosmic ray range. On the previously proposed M82 model (*2*) the average energy density of the electrons alone is in the range of 10^3 ev/cm^2, which is about 1000 times the energy density of the proton component of cosmic rays in the solar neighborhood of our own galaxy. Thus, on energy density arguments alone one might speculate that cosmic rays in our own galaxy may have originated in an event similar but less energetic than the explosion now occurring in M82.

A final word is necessary concerning the methods used in preparing the illustrations for this report. First, all reproductions are in negative form, that is, black stars against a light background. This technique is widely used in the preparation of astronomical prints intended to show threshold images because the eye detects a small increment of density much more readily against a light background than against a dark one.

Second, all reproductions except Fig. 1*a* are composite prints made from two or more superposed original negatives. Such prints gain over a single negative print in the detection of faint images for two reasons. (i) The signal-to-noise ratio increases by $N^{1/2}$ where N is the number of plates stacked together to make the composite. (ii) The contrast of the final print for threshold images is increased by N. The main disadvantage of superposition photography is that the increase in contrast, so essential to bring out the faint details, exceeds the latitude of the printing material to such an extent that detail is quickly lost in the bright parts of the image.

The problem can be overcome by the use of "masks" to control the gross density gradient over the area of an image. It is a refinement of the method of manual "dodging" during the printing operation to prevent over-exposure of bright areas and is more satisfactory because the images do their own dodging by "negative feedback" control.

An unsharp print of the printing positive is made on a suitable film or plate, with exposure and development time controlled to produce a density range which is the reverse of and slightly less than that of the printing positive. When registered with the positive and printed on high-contrast paper or film, the faint structural details of the image are retained without exceeding the latitude of the printing material.

In the case of Figs. 1*b*, 2, and 3, the density range of the combined images so far exceeds the latitude of the positive material that no amount of masking will retrieve detail in the brightest regions near the center. Hence no detail is visible in the nucleus of the galaxy. However, the masks have so greatly reduced the density gradient along the edges of the galaxy that detail has been held in areas that would otherwise have been completely black.

Since the masking technique has a progressive effect upon the image as one nears the bright portions of the galaxy, it is important to remember that no conclusions can be drawn from the illustrations in this report concerning the relative brightness of filaments at different distances from the galaxy.

ALLAN R. SANDAGE
WILLIAM C. MILLER
Mount Wilson and Palomar Observatories, Carnegie Institution of Washington, California Institute of Technology, Pasadena

References

1. C. R. Lynds, *Astrophys. J.* **134**, 659 (1961).
2. C. R. Lynds and A. R. Sandage, *ibid.* **137**, 1005 (1963).
3. H. M. Johnson, *Publ. Natl. Radio Astron. Obs.* **1**, No. 17 (1963).
4. A. Elvius, *Lowell Obs. Bull.* No. 19, 281 (1962).
5. T. A. Matthews and A. R. Sandage, *Astrophys. J.* **138**, 30 (1963).

6 March 1964

Fission Damage in Calcite and the Dating of Carbonates

Abstract. *Fission damage induced in calcite is shown by etch pits developed with weak acid at the damage sites. The damage can be differentiated from dislocations by annealing. By this method we have observed fossil fission damage in natural samples. Thus, some etch pits previously attributed to dislocations actually result from such damage. Annealing studies indicate that the damage should persist for about 4×10^7 years at 50°C, and direct evidence suggests that the fission damage has persisted for at least 10^6 years in one specimen.*

The discovery of fossil fission tracks in micas and glasses, and their use for dating these minerals correctly in many cases is a very significant development (*1, 2*), particularly since it is now known that etchable damage may be produced by fission fragments in other minerals, notably gypsum, quartz, and othoclase (*2*). Etch pits may be produced in such minerals as lithium fluoride by preferential chemical attack at the sites of damage produced by fission fragments penetrating the crystal (*3*). The dating of any mineral by a similar technique appears possible if (i) the

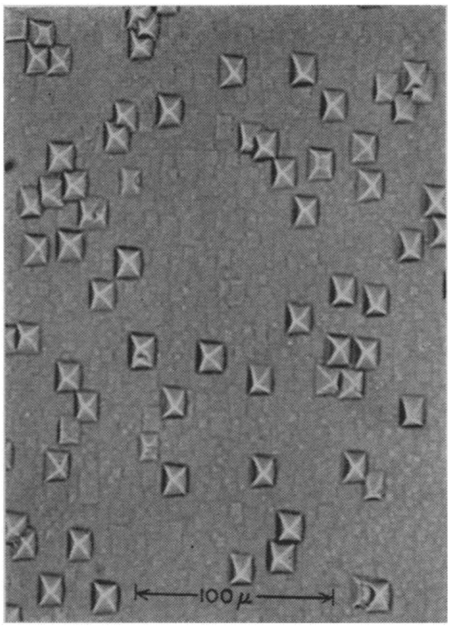

Fig. 1. Induced fission pits on calcite cleavage surface.

mineral contains sufficient uranium, (ii) the damage persists for geologically interesting periods of time, and (iii) the various minerals can be suitably prepared for treatment and examination. We have investigated fission damage in calcite by using cleaved surfaces of Iceland spar from various localities and have made the following observations.

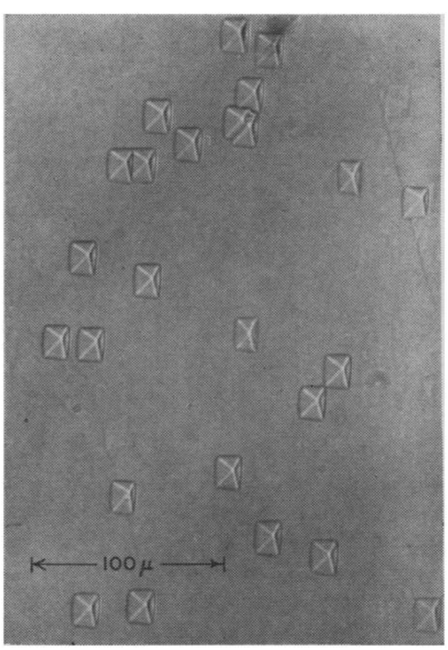

Fig. 2. Dislocation etch pits on calcite cleavage surface. This specimen was annealed for 18 hours at 400°C prior to etching to remove all fission damage. Regular shape of pits apparently characteristic of dislocation etch pits.

First of all, fission pits (etch pits at sites of fission damage) may be readily produced in calcite by Young's method (*3*) whereby the specimen is placed in contact with a film of U_3O_8 and then irradiated with thermal neutrons. Half of each calcite cleavage is shielded from the uranium by an aluminum foil to provide a blank surface for comparison. Fission fragments are produced by the thermal neutron fission of uranium-235. This is in contrast to fossil fission damage, which is virtually all produced by spontaneous fission of uranium-238. A wide variety of etching solutions may be used, such as acetic, formic, nitric, phosphoric, hydroxyacetic, and hydrochloric acids, the stronger acids being used in diluted form. These acids produce excellent fission pits, and, in fact, plain deionized water produces beautiful arrowhead-shaped fission pits after a period of 30 minutes. For our work we used concentrated formic acid. Specimens were immersed for 1 minute with agitation, then removed and blown dry in a blast of filtered compressed air. The etch pits produced are approximately rectangular in outline and pyramidal in shape. If Miller indices are assigned to the cleavage rhomb in such a way that the cleavage surface under examination is (100), then the long direction of the rectangular outline of the pits is $[01\bar{1}]$ and the short direction [011]. Figure 1 shows the fission pits produced by irradiation. The irradiated surface showed a much larger number of pits than the shielded end, an observation similar to that of Young for lithium fluoride (*3*). Although diverse shapes of fission pits may be produced by different etching solutions, and even by different dilutions of the same etchant, in all cases they were indistinguishable in general shape from the deep pits which formed on the unirradiated end of the crystal in much lower concentration.

The figures that are produced by etching on unirradiated calcite cleavage surfaces have been previously studied (*4*). Two distinct types of pits have been identified—deep sharp-bottomed pits which have been attributed to edge dislocations; and shallow, flat-bottomed pits attributed to point-defect clusters (*4*). It therefore appeared that fission pits could not be distinguished from dislocation pits by their general appearance.

We next performed annealing experiments to investigate the permanence of the fission damage. Heating irradiated specimens at 400°C before etching gave progressively weaker etch pits. After 1 hour the residual damage revealed by etching could not be mistaken for fission pits in an unannealed specimen. Similar annealing experiments were performed at lower temperatures; annealing at 250°C for 13 days gave approximately the same effect as did annealing for 10 minutes at 400°C, implying an activation energy of about 35 Kcal/mole. Upon extrapolation there is implication of significant healing of the fission damage in 44 million years at 50°C.

We next examined a number of unirradiated calcites and observed that the deep pits varied from a few hundred to a few thousand per square centimeter from specimen to specimen. In order to investigate the origin of these pits further we examined equivalent regions of pairs of matched cleavage surfaces. One-half was annealed at 400°C for 1 hour, and then both halves were etched. The two halves were compared both by photography and by scanning. In some cases all the pits were continuous across the cleavage surface. These we attributed to dislocations. In other cases a variable percentage of pits failed to develop on the heated half. These we attributed to fossil fission damage. The

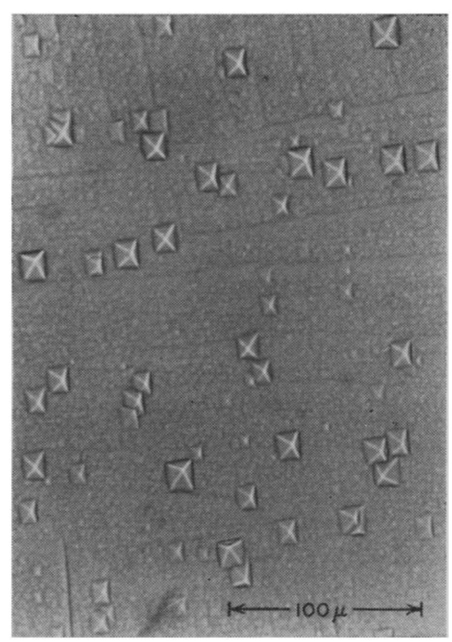

Fig. 3. Etch pits on yellow calcite. When other specimens of this material are annealed prior to etching, essentially all pits fail to develop. The pits shown here are thus attributed to fossil fission damage. Irregular shape is characteristic of fission pits. Compare induced fission pits in Fig. 2.

strongest evidence for fossil fission pits in calcite was presented by a calcite showing a pronounced yellow color, presumably color centers produced by radiation. This specimen showed 54,000 deep pits per square centimeter. Furthermore, the yellow color could obviously be correlated with the pit density. The end having much less color showed a greatly reduced number of pits. On annealing this specimen essentially all the deep pits failed to develop, leaving a concentration of only a few hundred pits per square centimeter. In the annealing the yellow color also faded.

We concluded that etching the cleavage faces of calcite produces deep pits both from dislocations and from fission damage and that the two can be distinguished by annealing experiments. One further piece of evidence supports this conclusion. A specimen of calcite showing a large number of dislocations was annealed for 18 hours at 400°C and then etched. This specimen should show only dislocation etch pits (Fig. 2) and may be compared with an etched specimen of the yellow calcite (Fig. 3) which should show almost all fission pits. The uniform shape of the presumed dislocation pits indicates a preferred direction of the dislocations. This may be controlled by a preferred growth direction or by the slip systems. In contrast, the fission damage trails will be inclined at all angles to the cleavage face and consequently will not give etch pits of uniform shape. Our interpretation is further strengthened by the fact that the presumed fossil fission pits vary in size (Fig. 3). This is understandable since the damage trails are distributed throughout the volume of the crystal. Those which almost transect the surface will not begin rapid growth until a slight amount of material is removed in the slowly dissolving direction perpendicular to the cleavage surface. Thus, such a pit will effectively be etched for a shorter total time. In contrast, the induced fission pits (Fig. 1) are of uniform size since, in this case, all the fission damage trails originate on the surface.

In addition to the indirect evidence from annealing experiments, an estimate for the durability of the fission damage was obtained from the yellow calcite by direct means. An analysis of this material showed it to contain 42 ± 3 parts of uranium per million (*5*). If we crudely estimate that the etching technique samples a region about 10 μ thick below the surface, we obtain an age of 2.5×10^6 years for this specimen. This is not an unreasonable age since the specimen came from the Chihuahua, Mexico, deposits which are thought to be associated with Tertiary or Quaternary volcanic activity (*6*). In any event the fission damage appears to have persisted for at least 10^6 years in this specimen.

ROBERT F. SIPPEL
EVERETT D. GLOVER
Socony Mobil Oil Company, Field Research Laboratory, Dallas, Texas

References and Notes

1. P. B. Price and R. M. Walker, *Nature* **196**, 732 (1962); R. L. Fleischer and P. B. Price, *J. Appl. Phys.* **34**, 2903 (1963); ———, Geol. Soc. Am. Meeting, New York City, 18–20 Nov. 1963; P. B. Price, R. L. Fleischer, D. S. Miller, E. S. Symes, *ibid.*
2. P. B. Price and R. M. Walker, *J. Geophys. Res.* **68**, 4847 (1963).
3. D. A. Young, *Nature* **182**, 375 (1958).
4. R. E. Keith and J. J. Gilman, *Acta Met.* **8**, 1 (1960).
5. We thank J. A. S. Adams for this measurement which he arranged to have done at Rice University.
6. C. Fries, Jr., *U.S. Geol. Surv. Bull.* **954-D**, 113 (1948).

31 January 1964

Electrokinetic Behavior of Ion-Exchange Resin

Abstract. *If a bed of ion-exchange beads immersed in water is subjected to a vertical electrical field of appropriate strength and polarity, vertical chains of beads are formed at the surface of the bed.*

An ion-exchange bead in water is a very large polyelectrolyte ion with small counterions. A bed of such beads is a good electrical conductor (*1*) with an unusual kind of flexibility which we shall describe.

The experiments which illustrate this behavior were carried out with 100- to 200-mesh (about 0.1 mm diameter) beads of polystyrene-divinyl benzene anion-exchange resin (Dowex 1-X8) in the chloride form, or cation-exchange resin (Dowex 50W-X8) in the hydrogen form. The resins were prepared by washing with dilute base and acid, and then by thorough washing with conductivity water. The resin beds were formed in a glass U-tube, or in a straight, vertical, glass tube, with platinum electrodes and with electrical fields of 0 to 25 v/cm in the water above the resin.

At a threshold of approximately 10 v/cm, the beads at one surface of a bed in the U-tube align into chains which rise vertically. A photograph of such chains is shown in Fig. 1. The chain height is roughly proportional to the applied electric field up to a limiting height of a few centimeters at 20 v/cm. At higher voltages the chains become unstable and lose small fragments which drift through the water and ultimately settle until they reach the surface of the bed or another chain. Cation-exchange resin chains form on the side of the anode, and anion-exchange resin chains on the side of the cathode. In a vertical tube chains are formed only if the appropriate electrode is above the bed. Mixed cation-exchange and anion-exchange beads do not form chains.

Each resin bead is a good electrical conductor because of its mobile ions, and the resin bed is also a good conductor because the beads are in contact. In an electrical field the bed is polarized. With a cation-exchanger the mobile counterions migrate toward the cathode, leaving the anode side negatively charged owing to the fixed charges. The electrophoresis of the beads toward the anode is opposed by gravity. A bead in a chain is supported by those below it and is more highly charged owing to polarization. If the field is strong enough to pull a fragment, perhaps a single bead, from the

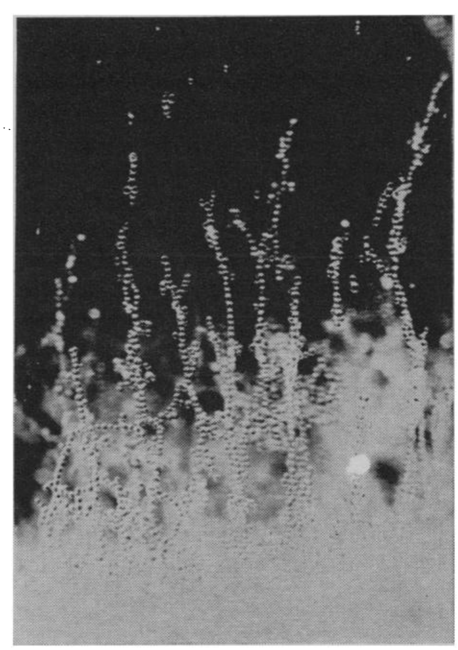

Fig. 1. Electrophoresis of anion-exchange resin particles in water in an electric field of 20 v/cm.